^{1}H NMR Sequential Assignments and Identification of Secondary Structural Elements in Oxidized Putidaredoxin, an Electron-Transfer Protein from *Pseudomonas*†

Xiao Mei Ye and Thomas C. Pochapsky*
Department of Chemistry, Brandeis University, Waltham, Massachusetts 02254
Susan Sondej Pochapsky
Bruker Instruments, Manning Park, Billerica, Massachusetts 01821
Received August 26, 1991; Revised Manuscript Received November 18, 1991

ABSTRACT: Sequential ^{1}H resonance assignments and secondary structural features of putidaredoxin (Pdx), a 106-residue globular protein consisting of a single polypeptide chain and a [2Fe–2S] cluster, are reported. No crystal structure has been obtained for Pdx or for any closely homologous protein. The sequentially assigned resonances represent ca. 83% of all the protons in Pdx and a large majority of those protons which are unaffected by the paramagnetism of the iron–sulfur cluster. A total of three α-helices, two β-sheets, and two type I β-turns have been identified from NOE (nuclear Overhauser effect) patterns. Besides the extensive β-sheet described previously, a second sheet is identified, consisting of two short antiparallel strands (Ile 89–Thr 91 and Val 21–Leu 23), one of which ends in a tight type I turn (Thr 91–Pro 92–Glu 93–Leu 94). One short helix (Ala 26–Gly 31) and a second longer helical region (Glu 54–Cys 73) are present. This second helical region is discontinuous, breaking at Pro 61, resuming at Glu 65, and ending at Cys 73. The functionally important C-terminal tryptophan residue has been identified, and some structural constraints on this residue are described. Previously reported functional data concerning Pdx are discussed in light of present structural information. Finally, approaches to the determination of a high-resolution solution structure of the protein are discussed.

An important aspect of biological electron transfer is the specificity often exhibited by physiological redox partners. A particularly instructive example of such specificity is to be found in cytochrome P-450$_{cam}$/putidaredoxin (Pdx)[1] couple. Pdx, a globular protein consisting of a single 106 residue polypeptide and a [2Fe–2S] prosthetic group, acts as a specific reductant for P-450$_{cam}$, a monooxygenase isolated from *Pseudomonas putida* grown on a medium containing camphor as the sole carbon source (Cushman et al., 1967). P-450$_{cam}$ catalyzes the first step in camphor catabolism, the 5-*exo*-hydroxylation of camphor by molecular oxygen. The hydroxylation requires two electrons for the reduction of molecular oxygen in the course of turnover. Pdx transfers these electrons in two discrete steps from the FAD-containing NADH-dependent Pdx reductase to P-450$_{cam}$. Pdx has also been shown to act as an effector for catalysis by P-450$_{cam}$. The ternary complex between fully reduced P-450$_{cam}$, O_2, and camphor is incapable of turnover in the absence of Pdx (Lipscomb et al., 1976; Shiro et al., 1989). Other [2Fe–2S] proteins (adrenodoxin and spinach ferredoxin) have been found to be incompetent for the effector role played by Pdx, although they reduce the P-450$_{cam}$/substrate complex efficiently. On the other hand, the one-iron-containing rubredoxin from *Clostridium pasteurianum* and mammalian hepatic cytochrome b_5 cannot act as reductants in this reaction, both having higher electrode potentials than the P-450$_{cam}$/substrate complex, but will serve as effectors for substrate turnover by the ternary complex (Tyson et al., 1972; Lipscomb et al., 1972; Geren et al., 1986).

The specificity of interaction between Pdx and P-450$_{cam}$ seems to be the result of a combination of electronic and structural factors. The enzyme/ligand interactions which control redox potential in P-450$_{cam}$ prevent reduction of substrate-free cytochrome by reduced Pdx (which might otherwise result in high concentrations of electron-deficient oxo species). These interactions have been described in detail (Sligar, 1976). Less is known concerning the structural features involved in protein–protein recognition. This lack is due in large part to the paucity of information concerning the tertiary structure of Pdx, since a high-resolution X-ray crystal structure of P-450$_{cam}$ has been published (Poulos et al., 1985, 1986, 1987). More recently, some structural information concerning Pdx has become available. The cysteine residues involved in ligation of the iron–sulfur cluster have been identified by site-directed mutagenesis experiments as Cys 39, Cys 45, Cys 48, and Cys 86 (Gerber et al., 1990). We have previously described the use of solution ^{1}H NMR methods to identify a five-strand β-sheet in the oxidized form of Pdx. Once identified, this extensive secondary structural feature permitted us to describe the folding topology of the protein (Pochapsky & Ye, 1991). Herein, we expand on those preliminary results by describing ^{1}H sequential assignments and identifying the

† This research was supported in part by a grant from the National Institutes of Health (GM-44191, T.C.P.). Acknowledgment is made to the Donors of the Petroleum Research Fund, administered by the American Chemical Society, for the partial support of this research.
* To whom correspondence should be addressed.

[1] Abbreviations: DSS, 2,2-dimethyl-2-silapentane-5-sulfonate; FAD, flavine adenine dinucleotide; fid, free induction decay; HOHAHA, homonuclear Hartmann–Hahn spectroscopy; JR, jump–return; NADH, nicotinamide adenine dinucleotide; NMR, nuclear magnetic resonance; NOE, nuclear Overhauser effect; NOESY, two-dimensional NOE spectroscopy; Pdx, putidaredoxin; 2Q, double quantum; 2QF-COSY, double-quantum filtered correlated spectroscopy.

0006-2960/92/0431-1961$03.00/0

major secondary structural features of oxidized Pdx.

Materials and Methods

Oxidized Pdx was isolated from bacterial cultures, purified, and prepared for spectroscopy as described previously (Gunsalus & Wagner, 1978; Pochapsky & Ye, 1991). Final concentrations of NMR samples were typically 5 mM as determined by optical spectroscopy. Samples were sealed in NMR tubes under argon in order to minimize sample degradation during long runs. NMR samples were prepared with 1 mM 2-hydroxyethanethiol as a preservative. This preparation method often yielded samples which showed little or no degradation as judged by one-dimensional ^{1}H NMR and optical spectroscopy after several days at 17 °C.

All NMR spectroscopy was performed at 17 °C, pH 7.4 (uncorrected for isotope effects). One- and two-dimensional NMR experiments were performed either on the LDB-500 500-MHz NMR spectrometer at Brandeis University built by A. Redfield and S. Kunz or on a Bruker AMX-600 600-MHz NMR spectrometer (Bruker Instruments, Billerica, MA). A spectral width of 8000 Hz in ω_2 was used on the LDB-500 for all experiments, with a digital resolution of 1024 complex points and zero-filling to 2048 complex points. Typically, 240 or 480 increments of t_1 were used. Phase sensitivity in the ω_1 dimension was obtained on the LDB-500 for all experiments using the method of States et al. (1982). Two-dimensional experiments described here which were performed on the LDB-500 include NOESY and NOESY-JR. The NOESY experiment was performed using a standard pulse sequence and phase cycling, with presaturation for water suppression when appropriate (Kumar et al., 1980; Billeter et al., 1982). The NOESY-JR experiment was performed in a similar manner (without presaturation of the water resonance), except that the observe $\pi/2$ pulse was replaced with a $\pi/2_x$–τ–$\pi/2_{-x}$ ("jump–return") semiselective pulse with the carrier placed on water in order to avoid excitation of the water resonance (Plateau & Gueron, 1982). A 100-ms mixing time was used in the NOESY and NOESY-JR experiments.

Experiments performed on the AMX-600 include 2QF-COSY, 2Q, HOHAHA, and NOESY. A spectral width of 10000 Hz in ω_2 was used on the AMX-600 for all experiments, with a digital resolution of 2048 complex points. The spectral width in ω_1 was also 10000 Hz for all experiments except for the 2Q experiment, in which case a spectral width of 20000 Hz in ω_1 was used. Phase sensitivity in the ω_1 dimension was obtained for all experiments on the AMX-600 using TPPI (time-proportional phase incrementation). A total of 400 increments of t_1 were used for the NOESY experiment, while 500 increments of t_1 were used for all coherence transfer experiments. Water suppression was obtained by presaturation of the water resonance. Typically, a mixing time of 100–200 ms was used in the NOESY experiment. 2QF-COSY and HOHAHA experiments were performed using standard sequences (Rance et al., 1983; Bax & Davis, 1985). The HOHAHA experiment was performed using a mixing time of 60 ms and a spin-lock field of 7.5 KHz. An MLEV-17 composite-pulse decoupling sequence was used for spin locking.

Processing for all data obtained on the LDB-500 was performed on a Silicon Graphics Iris/4D workstation using D. Hare's FELIX program. Data sets were zero-filled to 2048 complex points in t_2 prior to transformation, if required. Data acquired on the AMX-600 were processed on a Bruker X-32 computer using UXNMR software. A 45°-shifted sine bell over the appropriate time domain was used prior to transformation of coherence-transfer fids in which antiphase multiplets are observed as cross peaks (2QF-COSY and 2Q), while a Gaussian weighting function was used for apodization of NOESY and HOHAHA data. NOESY-JR data were treated with a 10-Hz convolution difference weighting function and a cosine bell prior to t_2 transformation. Transformation in t_1 was performed after zero-filling to 2048 complex points and application of a $\pi/4$-shifted since bell over the nonzero data points. The first data set ($t_1 = 0$) of all cosine-modulated experiments was multiplied by 0.5 in order to reduce t_1 noise (Otting et al., 1986), and a polynomial baseline-straightening function was applied to the data sets prior to t_1 transformation.

Results

Spin System Identification. The procedures used for spin system identification were described in a previous publication (Pochapsky & Ye, 1991). Only for those spin system types not reported previously will assignment methods be described here. Theoretically, spin systems of different amino acids may be identified by their characteristic patterns of chemical shifts and connectivities. Once such identifications are made, sequential NOEs are used to assign the spin systems sequence-specifically (Wüthrich, 1986). In practice, it proved to be more useful to concentrate initially on the identification of the secondary structural features of Pdx. After such identification was made, relatively few of the spin systems needed to be identified in order to assign backbone resonances uniquely (Saudek et al., 1989). In a few cases, spin system identification and sequential assignment were possible only after some tertiary structural constraints were obtained, after which ambiguous backbone connectivities could be verified.

The primary source of difficulty in obtaining and interpreting structural information from two-dimensional NMR spectra of oxidized Pdx is the presence of unpaired electron spin density at the iron–sulfur cluster under ambient conditions. Coupling of electronic and nuclear spins gives rise to rapid nuclear relaxation and severe broadening of the resonances of nearby nuclei. Oh and Markley reported that the resonances of protons closer than ca. 7.8 Å to either of the iron atoms in the oxidized form of *Anabaena* 7120 ferredoxin (as calculated from comparison with the known crystal structure of the *Spirulina* ferredoxin) were not observed in two-dimensional ^{1}H spectra (Oh & Markley, 1990). Preliminary structural calculations (vide infra) indicate that a similar distance dependence of the paramagnetic broadening is operant for oxidized Pdx.

Aliphatic Spin Systems. Seven out of a total of nine alanines in Pdx have been assigned. Only Ala 43 and Ala 46, which are in the region near iron–sulfur cluster, have not been identified. Thirteen of fourteen valines are assigned, with only Val 36 remaining unaccounted for, due also to its proximity to the Fe–S cluster. Most of the valine spin systems give rise to complete sets of cross peaks with the NH proton in HOHAHA spectra (τ_m = 60 ms, see Figure 1). Four leucine residues (Leu 15, Leu 23, Leu 78, and Leu 94) are assigned out of six in the protein. Leu 84 is sequentially and spatially close to one cysteinyl residue involved in ligation of the Fe–S cluster (Cys 86), while the side chain of Leu 71, for which only the NH proton has been assigned, is also apparently in close proximity to the cluster. Five isoleucine spin systems have been completely identified and sequentially assigned (Ile 32, Ile 68, Ile 88, Ile 89, and Ile 97). The spin system of Ile 35 has been partially assigned. The assignment of Ile 97 was reported previously (Pochapsky & Ye, 1991). Methionine residues, with spin systems topologically similar to glutamine, are most easily identified after sufficient nearby residues have been sequentially assigned to permit an unambiguous identification. There are three methionines in Pdx; Met 90 and Met 70 were

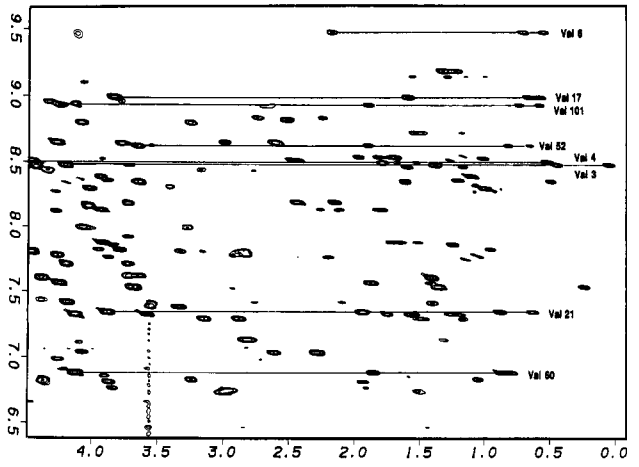

FIGURE 1: Portion of the 600-MHz ^{1}H HOHAHA spectrum of oxidized Pdx (τ_m = 60 ms) with the connectivity for eight valine spin systems between the NH proton (ω_2) and side-chain resonances delineated.

identified by sequential assignment; Met 24 is evidently in close proximity to the prosthetic group. Of the four proline residues in Pdx, Pro 61 and Pro 80 have been completely assigned, while portions of the Pro 92 and Pro 102 spin systems have been identified. In both of these cases, unambiguous assignment of the complete spin systems will require the use of heteronuclear-edited methods in order to resolve severe spectral overlap.

Aromatic Spin Systems. All three tyrosine residues in Pdx, Tyr 5, Tyr 33, and Tyr 51, have been identified (Pochapsky & Ye, 1991). The identification of the single phenylalanine residue, Phe 56, was also described previously. The aromatic spin system of Trp 106, the only tryptophan in Pdx, has been completely assigned by a combination of HOHAHA, 2QF-COSY, and NOESY data. There are two histidines in Pdx. The spin system of His 8 is identified by a HOHAHA peak between the $C_{\delta 2}H$ and $C_{\epsilon 1}H$ resonances, with NOE connectivities between the His 8 $C_\beta H_2$ and $C_{\delta 2}H$ confirming the assignment. The backbone protons of His 49 are not observed, as expected due to the proximity of the Fe–S cluster at Cys 48; however, one of the imidazole ring protons has been tentatively identified by NOE connectivities with nearby residues (e.g., Tyr 51, Val 74).

Hydrophilic and Charged Amino Acid Spin Systems. Five out of eight glycines in Pdx have been assigned, Gly 10, Gly 20, Gly 31, Gly 69, and Gly 96. The other three (Gly 37, Gly 40, and Gly 41) are in a loop of polypeptide which binds the iron–sulfur cluster and are not observed. Five of the seven serine residues in Pdx have been identified. The assignments of Ser 1 and Ser 82 were reported previously. The assignment of Ser 7 extends the β-sheet previously described. The NH of Ser 7 exchanges only slowly with solvent, and the $C_\alpha H$ of Val 6 overlaps with the HDO line, and so the expected strong Val 6–Ser 7 $C_\alpha H_i/NH_{i+1}$ NOE is observed in spectra obtained in D_2O solution. Four of the five threonines in Pdx are now assigned, with only Thr 47 remaining unassigned. The identification of threonine spin systems is straightforward using HOHAHA data and confirmed in most cases by the distinctive remote peaks in the 2Q spectrum at $C_\alpha H = \omega_2$, $(C_\beta H + NH) = \omega_1$.

Of the six cysteines in Pdx, four (Cys 39, Cys 45, Cys 48, and Cys 86) have been identified as binding the Fe–S cluster through covalent sulfide linkages to the two Fe atoms (Gerber et al., 1990). The backbone resonances of Cys 73 were identified by sequential assignment, followed by spin system identification from NOE and 2QF-COSY data. No assignment for Cys 85 can be made at present due to hyperfine interactions with the Fe–S cluster.

Pdx is a highly acidic protein with a total of 15 aspartate and glutamate residues. Eight aspartates have been identified and assigned out of a total of nine. The missing Asp 38 is adjacent to Cys 39, one of the prosthetic group ligands. All six glutamates have been identified; HOHAHA data provide connectivities from NH to $C_\alpha H$, $C_\beta H_2$, and $C_\gamma H_2$, while the $C_\beta H_2$ and $C_\gamma H_2$ can be distinguished from each other by the connectivity between $C_\alpha H$ and $C_\beta H_2$ resonances in the 2QF-COSY spectrum. The spin systems of asparagine and glutamine residues are identified in a similar manner. Differentiation between asparagine and aspartate is often obtained by NOE connectivity between the $C_\beta H_2$ protons of asparagine and a pair of mutually coupled exchangeable proton resonances which identify the $N_\delta H_2$ proton resonances. All four Asn's in Pdx have been assigned. The assignment of the glutamine spin system is in theory similar, but it proved somewhat more difficult in practice. Three glutamine spin systems (Gln 14, Gln 25, and Gln 105) have been identified out of total of four in the protein. The apparent proximity of the NH proton of Gln 25 to the iron–sulfur cluster prevents its identification, although the remainder of the spin system is identifiable by virtue of sequential NOEs to the NH of Ala 26 from the CαH and CβH_2 protons, which can then be connected to each other in coherence transfer spectra. The $N_\epsilon H_2$ protons were not identified for any of these spin systems in Pdx, presumably due to fast exchange of these protons with solvent. Glutamate and glutamine spin systems were therefore distinguished by sequential assignment.

All three lysines in Pdx are now assigned (Lys 2, Lys 59, and Lys 79). Lysine residues have long side chains and are assigned from both ends of the spin system. Connectivities between lysine $C_\epsilon H_2$ and $C_\delta H_2$ resonances are identified in the 2QF-COSY spectrum by their distinctive chemical shift relationships. The $C_\epsilon H_2$ also show connectivity with the $C_\gamma H_2$ in HOHAHA and NOESY, while the NH resonance has cross peaks with the $C_\alpha H$, $C_\beta H_2$, and $C_\gamma H_2$ in the same spectra. The assignment of all five arginines was accomplished in a similar manner. The $N_\epsilon H$ protons were identified by 2Q correlation with the $C_\delta H_2$ protons, as distinctive remote connectivities are observed in the double-quantum spectrum at $N_\epsilon H = \omega_2$, $C_{\delta 1}H + C_{\delta 2}H = \omega_1$. The $N_{\eta 1}H_2$ and $N_{\eta 2}H_2$ protons of Arg 13 and Arg 83 have been identified on the basis of sets of intense NOEs between the $N_\epsilon H$ proton of each spin system and pairs of broad exchangable proton resonances.

Sequential Assignments. The present communication expands on sequential assignments described previously (Pochapsky & Ye, 1991). Only those assignments not discussed in the previous paper will be described here. Sequence-specific ^{1}H resonance assignments are summarized in Table I, and the fingerprint region of the 600-MHz ^{1}H 2QF-COSY spectrum, with the sequential assignments of the NH/C_αH cross peaks, is shown in Figure 2. Not shown is the 2Q spectrum, in which connectivities between NH and $C_\alpha H$ protons which overlap with the water resonance are observable (Otting & Wüthrich, 1986). It is our belief that the assignments listed in Table I are the most complete possible using homonuclear two-dimensional NMR methods and that further assignments will only be possible using heteronuclear-edited three-dimensional NMR techniques. The gene for Pdx has been cloned (Koga et al., 1989), and current efforts in our laboratory are directed toward expressing isotopically labeled Pdx for this purpose (L. Rost, R. Baggio, G. Ratnaswamy, A. Patera, R. Williams, and

Table I: ^{1}H Resonance Assignments for Oxidized Pdx, pH 7.4, 17 °C[a]

Ser 1 $C_\alpha H$ 3.88; $C_\beta H_2$ 3.40, 3.57
Lys 2 NH 9.15; $C_\alpha H$ 4.58; $C_\beta H_2$ 1.29, 1.55; $C_\gamma H_2$ 1.12, 1.00; $C_\delta H_2$ 1.25, 1.38; $C_\epsilon H_2$ 2.65
Val 3 NH 8.48; $C_\alpha H$ 4.18; $C_\beta H$ 1.38; $C_\gamma H_3$ 0.04, 0.45
Val 4 NH 8.50; $C_\alpha H$ 4.40; $C_\beta H$ 1.78; $C_\gamma H_3$ 0.495, 0.53
Tyr 5 NH 8.84; $C_\alpha H$ 4.72; $C_\beta H_2$ 2.23, 2.72; $C_\delta H$ 6.48; $C_\epsilon H$ 6.05; OH 8.02
Val 6 NH 9.50; $C_\alpha H$ 4.68; $C_\beta H$ 2.18; $C_\gamma H_3$ 0.56, 0.72
Ser 7 NH 8.95; $C_\alpha H$ 4.31; $C_\beta H$ 3.78
His 8 NH 7.54; $C_\alpha H$ 4.23; $C_\beta H_2$ 2.90, 3.10; $C_{\delta 2} H$ 7.15; $N_{\delta 1} H$ 9.45; $C_{\epsilon 1} H$ 7.92
Asp 9 NH 7.41; $C_\alpha H$ 4.18; $C_\beta H_2$ 2.09, 2.75
Gly 10 NH 7.99; $C_\alpha H_2$ 3.27, 4.05
Thr 11 NH 7.81; $C_\alpha H$ 3.78; $C_\beta H$ 3.94; $C_\gamma H_3$ 0.95
Arg 12 NH 8.72; $C_\alpha H$ 4.58; $C_\beta H_2$ 1.46, 1.53; $C_\gamma H_2$ 1.17; $C_\delta H_2$ 2.89, 3.12; $N_\epsilon H$ 7.29
Arg 13 NH 8.49; $C_\alpha H$ 4.45; $C_\beta H_2$ 1.66, 1.66; $C_\gamma H_2$ 1.30, 1.51; $C_\delta H_2$ 2.97, 3.02; $N_\epsilon H$ 6.74; $N_{\eta 1} H_\infty$ 6.23; $N_{\eta 2} H_2$, 7.20
Gln 14 NH 8.55; $C_\alpha H$ 5.10; $C_\beta H_2$ 1.68, 1.68; $C_\gamma H_2$ 1.82, 1.97
Leu 15 NH 9.19; $C_\alpha H$ 4.54; $C_\beta H_2$ 1.31, 1.23; $C_\gamma H$ 1.31; $C_\delta H_3$ 0.52, 0.60
Asp 16 NH 8.19; $C_\alpha H$ 4.71; $C_\beta H_2$ 2.14, 2.42
Val 17 NH 8.99; $C_\alpha H$ 3.81; $C_\beta H$ 1.58; $C_\gamma H_3$ 0.58, 0.66
Ala 18 NH 8.40; $C_\alpha H$ 3.92; $C_\beta H_3$ 1.10
Asp 19 NH 7.77; $C_\alpha H$ 3.88; $C_\beta H_2$ 2.19, 2.42
Gly 20 NH 8.80; $C_\alpha H_2$ 3.23, 4.08
Val 21 NH 7.34; $C_\alpha H$ 3.87; $C_\beta H$ 1.93; $C_\gamma H_3$ 0.62, 0.89
Ser 22 NH 8.75; $C_\alpha H$ 5.18; $C_\beta H_2$ 3.72, 4.22
Leu 23 NH 8.38; $C_\alpha H$ 3.90; $C_\beta H_2$ 1.70; $C_\gamma H$ 1.65; $C_\delta H_3$ 0.52, 0.57
Gln 25 $C_\alpha H$ 3.63; $C_\beta H_2$ 1.80; $C_\gamma H$ 2.34
Ala 26 NH 7.87; $C_\alpha H$ 3.82; $C_\beta H_3$ 1.23
Ala 27 NH 6.81; $C_\alpha H$ 3.23; $C_\beta H_3$ 1.04
Val 28 NH 8.18; $C_\alpha H$ 3.71; $C_\beta H$ 1.90; $C_\gamma H_3$ 0.68, 0.75
Ser 29 NH 7.71; $C_\alpha H$ 4.18; $C_\beta H_2$ 3.71
Asn 30 NH 7.03; $C_\alpha H$ 4.69; $C_\beta H_2$ 2.60, 2.28; $N_\gamma H_2$ 7.05, 8.41
Gly 31 NH 7.39; $C_\alpha H_2$ 3.33, 3.55
Ile 32 NH 7.51; $C_\alpha H$ 3.68; $C_\beta H$ 1.37; $C_{\gamma 1} H_3$ 0.23; $C_{\gamma 2} H_2$ 0.39, 0.65; $C_{\delta 2} H_3$ −0.02
Tyr 33 NH 6.96; $C_\alpha H$ 4.25; $C_\beta H_2$ 2.71, 2.88; $C_\delta H_2$ 6.93; $C_\epsilon H_2$ 6.67
Asp 34 NH 9.47; $C_\alpha H$ 4.09; $C_\beta H_2$ 2.43, 2.50
Ile 35 NH 7.41; $C_\alpha H$ 3.50; $C_\beta H$ 1.39; $C_{\gamma 1} H_3$ 0.40
His 49 $C_\epsilon H$ (7.22)
Val 50 NH 8.92; $C_\alpha H$ 4.12; $C_\beta H$ (1.78); $C_\gamma H_3$ (0.38), (0.71)
Tyr 51 NH 8.95; $C_\alpha H$ 4.96; $C_\beta H_2$ 2.62, 2.69; $C_\delta H_2$ 6.63; $C_\epsilon H_2$ 6.65
Val 52 NH 8.61; $C_\alpha H$ 3.63; $C_\beta H$ 1.89; $C_\gamma H_3$ 0.66, 0.81
Asn 53 NH 8.26; $C_\alpha H$ 4.28; $C_\beta H_2$ 2.57, 2.79; $N_\gamma H_2$ 8.04, 7.08
Glu 54 NH 9.09; $C_\alpha H$ 4.04; $C_\beta H_2$ 1.85, 1.88; $C_\gamma H_2$ 2.14
Ala 55 NH 8.30; $C_\alpha H$ 4.00; $C_\beta H_3$ 1.00
Phe 56 NH 8.66; $C_\alpha H$ 4.26; $C_\beta H_2$ 2.57, 2.98; $C_\delta H$ 6.96; $C_\epsilon H$ 7.10; $C_\xi H$ 7.00
Thr 57 NH 7.33; $C_\alpha H$ 3.58; $C_\beta H$ 4.025; $C_\gamma H_3$ 1.11; OH 5.35
Asp 58 NH 8.52; $C_\alpha H$ 4.45; $C_\beta H_2$ 2.455, 2.46
Lys 59 NH 7.32; $C_\alpha H$ 4.12; $C_\beta H_2$ 1.56, 1.73; $C_\gamma H_2$ 1.25, 1.20; $C_\delta H_2$ 1.49, 1.32; $C_\epsilon H_2$ 2.74
Val 60 NH 6.88; $C_\alpha H$ 4.11; $C_\beta H$ 1.86; $C_\gamma H_3$ 0.80, 0.87
Pro 61 $C_\alpha H$ 4.13; $C_\beta H_2$ 2.18, 1.71; $C_\gamma H_2$ 1.84, 1.97; $C_\delta H_2$ 3.44, 3.84
Ala 62 NH 8.36; $C_\alpha H$ 3.88; $C_\beta H_3$ 1.21
Ala 63 NH 8.53; $C_\alpha H$ 3.89; $C_\beta H_3$ 1.01
Asn 64 NH 8.45; $C_\alpha H$ 4.57; $C_\beta H_2$ 2.75, 3.15; $N_\delta H_2$ 6.47, 7.48
Glu 65 NH 8.48; $C_\alpha H$ 3.71; $C_\beta H_2$ 1.83; $C_\gamma H_2$ 2.09
Arg 66 NH 7.88; $C_\alpha H$ 3.90; $C_\beta H_2$ 1.63, 1.70; $C_\gamma H_2$ 1.52; $C_\delta H_2$ 2.99, 3.01
Glu 67 NH 8.09; $C_\alpha H$ 4.04; $C_\beta H_2$ 1.61; $C_\gamma H_2$ 2.00
Ile 68 NH 8.29; $C_\alpha H$ 3.40; $C_\beta H$ 1.61; $C_{\gamma 1} H_3$ 0.72; $C_{\gamma 2} H_2$ 0.92, 1.36; $C_{\delta 2} H_3$ 0.52
Gly 69 NH 7.62; $C_\alpha H_2$ 3.62, 3.71
Met 70 NH 7.42; $C_\alpha H$ 4.37
Leu 71 NH 8.38
Glu 72 NH 6.77; $C_\alpha H$ 3.83; $C_\beta H_2$ 1.92; $C_\gamma H_2$ 2.13, 2.36
Cys 73 NH 7.80; $C_\alpha H$ 4.49; $C_\beta H_2$ 2.89, 3.15
Val 74 NH 7.11; $C_\alpha H$ 4.09; $C_\beta H$ 1.68; $C_\gamma H_3$ 0.37, 0.68
Thr 75 NH 8.16; $C_\alpha H$ 4.02; $C_\beta H$ 3.80; $C_\gamma H_3$ 0.97
Ala 76 NH 7.62; $C_\alpha H$ 4.38; $C_\beta H_3$ 1.41
Glu 77 NH 7.91; $C_\alpha H$ 3.71; $C_\beta H_2$ 1.58, 1.81; $C_\gamma H_2$ 2.09
Leu 78 NH 8.49; $C_\alpha H$ 4.41; $C_\beta H_2$ 1.58, 1.59; $C_\gamma H$ 1.17; $C_\delta H_3$ 0.67, 0.82
Lys 79 NH 9.71; $C_\alpha H$ 4.80; C_βH2 1.58, 1.73; $C_\gamma H_2$ 0.93, 1.07; $C_\delta H_2$ 1.81, 1.95; $C_\epsilon H_2$ 2.28, 2.28
Pro 80 $C_\alpha H$ 4.24; $C_\beta H_2$ 2.28, 1.76; $C_\gamma H_2$ 2.14, 1.83; $C_\delta H_2$ 3.52, 3.70
Asn 81 NH 8.62; $C_\alpha H$ 4.68; $C_\beta H_2$ 2.58, 2.71; $N_\gamma H_2$ 6.545, 7.45
Ser 82 NH 7.98; $C_\alpha H$ 5.03; $C_\beta H_2$ 3.95, 4.00; OH 10.10
Arg 83 NH 9.37; $C_\alpha H$ 4.65; $C_\beta H_2$ 1.02, 1.05; $C_\gamma H_2$ 1.56, 1.22; $C_\delta H_2$ 3.08, 3.39; $N_\epsilon H$ 10.29; $N_{\eta 1} H_2$ 5.50; $N_{\eta 2} H_2$ 8.37
Ile 88 NH 6.84; $C_\alpha H$ 3.88; $C_\beta H$ 1.56; $C_{\gamma 1} H_3$ 0.47; $C_{\gamma 2} H_2$ 0.64, 1.34; $C_{\delta 2} H_3$ 0.35
Ile 89 NH 8.37; $C_\alpha H$ 3.625; $C_\beta H$ 1.60; $C_{\gamma 1} H_3$ 0.49; $C_{\gamma 2} H_2$ 1.08, 1.12; $C_{\delta 2} H_3$ 0.33
Met 90 NH 8.12; $C_\alpha H$ 4.26; $C_\beta H_2$ 1.58, 2.115
Thr 91 NH 7.10; $C_\alpha H$ 4.53 $C_\beta H$ 4.40; $C_\gamma H_3$ 1.04
Pro 92 $C_\alpha H$ 4.28; $C_\delta H_2$ 3.61, 3.64
Glu 93 NH 8.13; $C_\alpha H$ 3.92; $C_\beta H_2$ 1.81, 1.82; $C_\gamma H_2$ 2.14, 2.26
Leu 94 NH 7.56; $C_\alpha H$ 4.23; $C_\beta H_2$ 1.39, 1.88; $C_\gamma H$ 1.57; $C_\delta H_3$ 0.60, 0.78
Asp 95 NH 8.17; $C_\alpha H$ 3.89; $C_\beta H_2$ 2.48, 2.74
Gly 96 NH 9.64; $C_\alpha H_2$ 2.82, 4.02

Table I (Continued)

Ile 97 NH 7.77; $C_\alpha H$ 1.03; $C_\beta H$ 1.33; $C_{\gamma 1}H_3$ 0.64; $C_{\gamma 2}H_2$ 0.53, 1.34; $C_{\delta 2}H_3$ 0.31
Val 98 NH 4.88; $C_\alpha H$ 4.48; $C_\beta H$ 1.39; $C_{\gamma}H_3$ 0.61, 0.75
Val 99 NH 8.59; $C_\alpha H$ 4.75; $C_\beta H$ 1.48; $C_{\gamma}H_3$ 0.30, 0.36
Asp 100 NH 8.82; $C_\alpha H$ 5.28; $C_\beta H_2$ 2.50, 2.50
Val 101 NH 8.96; $C_\alpha H$ 4.23; $C_\beta H$ 1.88; $C_{\gamma}H_3$ 0.58, 0.72
Pro 102 $C_\alpha H$ 4.50; $C_\beta H_2$ 2.02, 1.72; $C_{\gamma}H_2$ 1.91; $C_{\delta}H_2$ 3.54
Asp 103 NH 8.64; $C_\alpha H$ 3.76; $C_\beta H_2$ 1.60, 2.18
Arg 104 NH 6.815; $C_\alpha H$ 4.37; $C_\beta H_2$ 1.59; $C_{\gamma}H_2$ 1.31; $C_{\delta}H_2$ 2.78, 2.83; $N_\epsilon H$ 7.13
Gln 105 NH 8.43; $C_\alpha H$ 4.34; $C_\beta H_2$ 0.97; $C_{\gamma}H_2$ 2.33, 1.44
Trp 106 NH 7.84; $C_\alpha H$ 4.46; $C_\beta H_2$ 2.82, 3.32, $C_{\delta 1}H$ 7.06 $C\epsilon_3 H$ 7.56; $N_{\epsilon 1}H$ 10.04; $C_{\xi 3}H$ 6.90; $C_{\xi 2}H$ 7.20; $C_\eta H$ 6.92

[a] Assignments are not stereospecific. All chemical shifts are in ppm relative to external standard DDS. Assignments shown in parentheses are tentative due to paramagnetic broadening which prevents observation of coherence transfer.

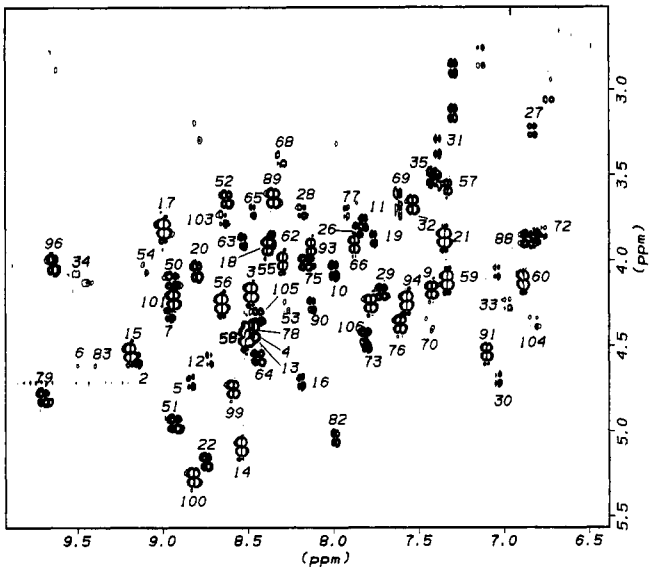

FIGURE 2: Fingerprint region of the 600-MHz 2QF-COSY spectrum showing sequential identification of NH–CαH cross peaks. Numbers refer to the sequence position as indicated in Table I.

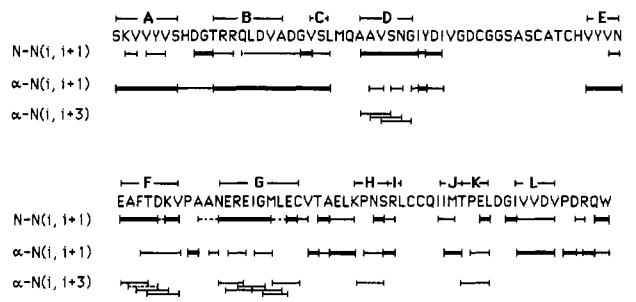

FIGURE 3: Sequential NOEs observed in oxidized Pdx. The relative intensities of NOEs are indicated by line thickness. Dotted lines represent NOEs expected but not identified due to spectral overlap. CαH_i/NH_{i+3} NOEs were not observed due to overlap for Phe 56–Lys 59 and Glu 65–Ile 68, but CαH_i/CβH_{i+3} NOEs were observed in these cases, and it is these NOEs which the denoted connectivity indicates. Boldface capital letters above the polypeptide chain cross-reference with the diagram shown in Figure 4.

T. Pochapsky, unpublished results).

The region from Ser 7 to Arg 13 was initially identified as Ser–X–Asp–Gly–Thr–X–X, which is unique in the protein sequence. Subsequent spin system identification completed the assignment of this segment of the polypeptide chain. Ala 18–Ser 22 was originally assigned as Ala–X–Gly–Val–X; Ser 22 has somewhat broadened side-chain resonances, due most likely to proximity to the Fe–S cluster. Only the NH proton of Leu 23 could be identified by sequential connectivity, while the Met 24 side chain remains unidentified, also probably due to paramagnetic broadening. As noted above, the side-chain spin system of Gln 25 is identifiable by sequential NOEs to the NH proton of Ala 26 and the expected HOHAHA and 2QF-COSY connectivities. The assignment of Ala 26–Ile 35 was begun from the segment Ala 26–Ala 27–Val 28, which is unique and readily identified. The remainder of this region of the polypeptide was assigned by clear sequential NOESY connectivities. Sequential assignment of the region from Glu 54 to Val 60 was begun at Phe 56, the only phenylalanine in the protein. The assignment of segment Pro 61–Cys 73 was started from Pro 61–Ala 62–Ala 63–Asp 64, which is unique. The remainder of this segment was assigned by the combination of sequential NOESY connectivities and spin system topologies. The segment Asp 64–Cys 73 is helical (vide infra), and the side of the helix which faces the interior of the protein is apparently close to the Fe–S cluster, making some side-chain assignments in this region problematic.

The segment Ile 88–Gly 96 was first assigned as X–Ile–X–Thr–Pro–X–X–X–Gly. Glu 93 was assigned by sequential connectivity and later confirmed by identification of spin system topology. The resonances of side-chain protons of Ile 88 are overlapped in many places with other resonances but were assigned by side-chain NOE connectivities with the spin system of Ile 89 and later confirmed by spin system topology. Leu 94, Asp 95, and Gly 96 were assigned by combination of sequential connectivity and spin system identification.

Near the C-terminus, Trp 106 was identified by NOEs between the distinctive indole spin system protons and the $C_\beta H_2$, $C_\alpha H$, and NH resonances, which in turn show mutual coherence transfer in 2QF-COSY and HOHAHA spectra. The spin system of Gln 105 could then be assigned by virtue of a strong sequential NOE from its NH to the NH of Trp 106. The spin system of Asp 103 was assigned by sequential NOE between its NH and the $C_\alpha H$ of Pro 102. Pro 102 was identified in part by NOE between the $C_\delta H_2$ of Pro 102 and the $C_\alpha H$ of Val 101. The spin system of Arg 104 was readily identified, but its sequential assignment was complicated by the overlap of the expected sequential NOE from its $C_\alpha H$ with the NH of Gln 105; however, sequential NOEs from Asp 103 permit the assignment to be made.

Identification of Secondary Structure. Regular secondary structural features in protein structures are identifiable by distinctive sequential NOE patterns. β-Sheet structure gives rise to strong CαH_i/NH_{i+1}, strong CβH_i/NH_{i+1}, and very weak or nonexistent NH_i/NH_{i+1} NOEs. Parallel and antiparallel strand orientations are distinguishable by a series of distinctive interstrand NOEs, most notably the strong CαH_i/CαH_j NOEs observed between antiparallel strands. Significant downfield NH chemical shifts and slow NH proton exchange with solvent are also common features of β-sheets, due to the networked hydrogen-bonding patterns present. Slow exchange is also often observed in β-turns for the NH proton of residue IV of the turn due to hydrogen bonding with the carbonyl oxygen of residue I. α-Helices give rise to strong NH_iNH_{i+1} NOEs, medium to weak NH_i/NH_{i+2}, and medium CαH_i/NH_{i+1},

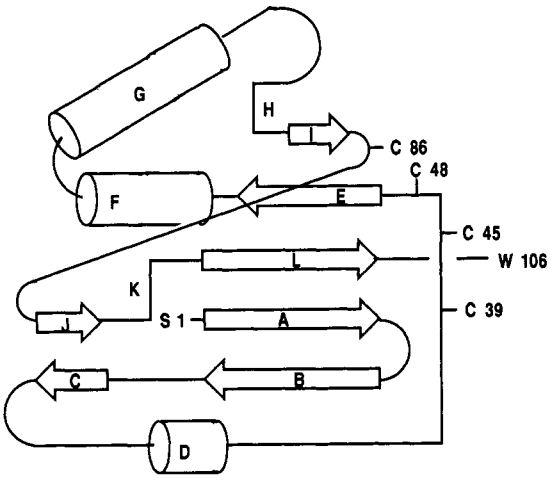

FIGURE 4: Schematic representation of secondary structure in oxidized Pdx. Cylindrical structures represent α-helices, broad arrows correspond to β-strands, and H and K represent tight turns. Letters correspond to boldface lettering scheme for the primary structure shown in Figure 3. The approximate relationship of the secondary structural elements to the four cysteinyl ligands of the iron–sulfur cluster as identified by mutagenesis (Gerber et al., 1990) are shown, as well as to the N- and C-terminal residues Ser 1 and Trp 106. No tertiary structural information is implied in this figure other than for the relative positions of β-strands in the two β-sheets.

$C_\alpha H_i/NH_{i+3}$, and $C_\alpha H_i/C_\beta H_{i+3}$ NOEs.

Sequential NOEs used to identify secondary structural motifs in Pdx are shown in Figure 3. Secondary structural domains are cross-identified in Figures 3 and 4. Two β-sheets have been identified in Pdx (see Figure 5). The larger sheet, consisting of five short strands (segments A, B, E, I, and L, Figures 3 and 4) with one parallel and three antiparallel strand orientations, was described in detail in a previous publication (Pochapsky & Ye, 1991). More complete sequential assignments have permitted identification of additional residues which take part in forming this sheet; it is now shown to contain residues Ser 7, Thr 11, Arg 12, and Arg 13 (segments A and B, see Figure 5), besides those residues originally assigned. Three residues, His 8, Asp 9, and Gly 10, form a short loop connecting strands A and B. This loop is characterized by three intense NH_i/NH_{i+1} NOEs (Figure 3). The amide protons of Ser 7 and Arg 13 exchange slowly with solvent, indicating that they take part in the hydrogen-bonding network defining the β-sheet.

The other, smaller β-sheet consists of a pair of two-residue antiparallel segments, C and J. Segment J, consisting of Ile 89 and Met 90, precedes a second tight turn, K, consisting of four residues, Thr 91–Pro 92–Glu 93–Leu 94. Like the previously described turn H (Lys 79–Pro 80–Asn 81–Ser 82), NOE patterns indicate that turn K adopts a type I configuration (see Figure 5). Strand C, consisting of Val 21 and Ser 22, is connected by a loop of three residues (Ala 18–Asp 19–Gly 20) to strand B of the larger β-sheet.

Three distinct α-helical structures have been identified in this protein. Residues Ala 26–Gly 31 form at least a short section of regular α-helix, marked D in Figures 3 and 4. Strong NH–NH connectivity between adjacent residues Gly 31–Ile 32–Tyr 33–Asp 34–Ile 35 as well as interdomain NOEs indicate that these residues probably occupy a compact structure. However, the distinctive $i/i+3$ NOEs which distinguish α-helical structures are not observed. The apparent proximity of residues Leu 23–Met 24–Gln 25 to the iron–sulfur cluster makes it difficult to establish whether any of these residues also take part in the formation of helix D.

Another α-helical region, F, is formed by residues Glu 54–Val 60. This helix begins immediately at the C-terminal end of β-strand E. Pro 61 acts to break helix F, which is then connected by a short loop formed by residues Ala 62 and Ala 63 to an α-helix formed by residues Asn 64–Cys 73, helix G. Residues Val 74–Ala 76 forms a loop linking this helix to a type I β-turn, H, which forms the edge of the larger β-sheet described previously.

Discussion

Pdx was first identified as a component of the P-450$_{cam}$ monooxygenase system over 20 years ago. Since that time, much has been learned concerning the stoichiometry and kinetics of the interaction between Pdx and its physiological

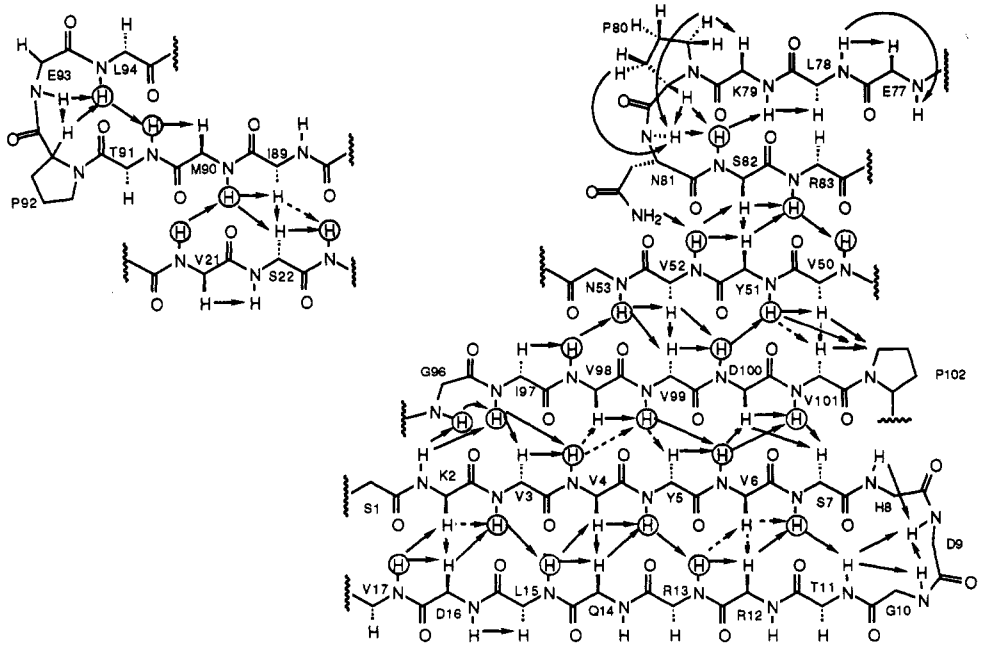

FIGURE 5: Two β-sheets in Pdx, as detailed by observed intra- and interstrand NOEs. The larger sheet was described previously (Pochapsky & Ye, 1991) but is now shown to be more extensive by further assignments. Residues are labeled with the standard one-letter amino acid code. Solid arrows represent observed NOEs, while dotted arrows represent expected NOEs which could not be verified due to spectral overlap. Circled NH protons are those observed to be at slow exchange with water in NOESY spectra obtained in D_2O.

redox partners, Pdx reductase and P-450$_{cam}$. The availability of the present structural information makes some interpretation of earlier observations appropriate.

Environment of Trp 106. The C-terminal Trp 106, the only tryptophan residue in Pdx, has been implicated in the electron transfer between Pdx and P-450$_{cam}$. Mutagenesis studies in which the C-terminal residue was replaced or deleted indicate that, while structurally nonessential (mutant proteins are expressed with the iron–sulfur cluster intact and with reduction potentials only marginally affected), Trp 106 is important to biological activity. Replacement of Trp 106 with Phe or Tyr results in proteins with reduced but measurable ability to transfer electrons to P-450$_{cam}$. Nonaromatic replacements for Trp 106 (Val, Lys, Leu, or Asp) result in reduction rates which are close to the background levels expected under the conditions of the experiment (Davies et al., 1990). It is unclear whether the aromatic character of this residue is important for the extended π orbital (as a potential pathway for electron transfer) or for the steric rigidity inherent in aromatic side chains, which may stabilize a particular binding mode between redox partners necessary for electron transfer. Present NMR data (particularly, rapid loss of the indole $N_\epsilon H$ proton signal upon solution of Pdx in D_2O) support the suggestion of previous studies that Trp 106 is in fact solvent exposed in the uncomplexed protein (Sligar et al., 1974). A strong NH–NH cross peak with Gln 105 suggests that the conformation of the backbone at this point is not extended, which would give rise to strong $C_\alpha H_i/NH_{i+1}$ and weak NH_i/NH_{i+1} sequential NOEs. Relatively few NOEs are observed to the Trp 106 side chain, with only one significant nonsequential NOE having been identified, from one of the $C_\gamma H_3$ groups of Val 98 to the $N_\epsilon H$ and $C_\delta H$ indole protons. Val 98 was identified previously as a constituent of the large β-sheet. On the basis of sheet geometry, the side chain of Val 98 faces the solvent as part of a "hydrophobic patch" which may play a role in protein–protein recognition (Pochapsky & Ye, 1991).

A further observation which has been made in connection with the C-terminal residue is the existence of two forms of Trp 106 in aged samples of protein. Samples of Pdx which have been kept at or near room temperature for extended periods of time often develop a second set of tryptophan indole resonances, the chemical shifts of which are almost exactly those of free tryptophan and line widths of which are suggestive of a small molecule. These same samples also exhibit a doubling of some resonances in the large β-sheet, most notably resonances assigned to Val 50, Tyr 51, Val 101, and Pro 102, which are spatially near to the C-terminus. SDS–PAGE gels of these samples give rise to two closely spaced bands, differing in molecular mass by several hundred daltons. Also observed is a small peptide fragment which appears to be of the correct size to be the result of cleavage of the larger species to the smaller molecular weight band. These observations point to a selective proteolysis which results in C-terminal heterogeneity of Pdx, which in turn may explain the lack of success in crystallizing this protein. It is interesting to note that C-terminal heterogeneity has been documented in adrenodoxin, with which Pdx shares significant sequence homology (Bhasker et al., 1987). At present, the mechanism of this proteolysis is not clear; scrupulous exclusion of oxygen seems to slow the appearance of the doubled resonances, which may indicate that an oxidative modification is responsible. The presence of trace amounts of a protease which copurifies with Pdx is also not ruled out.

Surface Carboxylates. Another structural feature of Pdx with implications for biological activity is the high density of negative charge present. Pdx contains a total of 15 Asp and Glu residues, as well as the C-terminal carboxylate. Geren and co-workers showed that modification of the carboxylates of Pdx with a carbodiimide reagent resulted in a loss of Pdx reductase reactivity (Geren et al., 1986). The most heavily modified carboxylates were found to be Asp 58 and glutamate residues 65, 67, 72, and 77. Residue 58 is found on helix F, while residues 65, 67, and 72 are on helix G. Glu 77 is part of the loop connecting helix G to the β-turn H. At the present level of structural analysis, there is no obvious pattern of charge asymmetry, as has been found for P-450$_{cam}$ and cytochrome *c*. However, residues 65, 67, 72, and 77 are all required by the folding topology (Figure 4) to be near the end of the molecule containing the Fe–S cluster. Furthermore, the helix containing residues 65, 67, and 72 contains a number of residues (Met 70 and Leu 71, in particular) the resonances assigned to which are quite broad, indicating proximity to the Fe–S center. As such, helix G and the ensuing loop may provide a negatively charged surface for docking interactions with redox partners in order to bring the redox centers into proximity. It is interesting to note that cytochrome b_5, which exhibits some ability to replace Pdx as an effector for turnover in the P-450$_{cam}$ system (vide supra) also contains helical structures bearing significant negative charge (Mathews, 1971). Recent studies indicate that Pdx competitively inhibits the binding between P-450$_{cam}$ and cytochrome b_5, suggesting that the two proteins bind to P-450$_{cam}$ at the same site (Stayton et al., 1989). These same workers also showed that loss of positive charge on the surface of P-450$_{cam}$ results in a decrease in binding interactions between P-450$_{cam}$ and cytochrome b_5 (Stayton & Sligar, 1990). On the basis of this collected evidence, it is tempting to speculate that negative charges on and nearby helix G may be involved in the effector activity.

Tertiary Structural Calculations. Despite the lack of complete ^1H assignments for the oxidized form of Pdx, enough secondary and tertiary structural constraints are available to begin preliminary structural analysis. Extensive data in the form of NOEs and coupling constant constraints are available for the hydrophobic core and regions of protein removed from the iron–sulfur prosthetic group. Overall sequence homology between Pdx and other [2Fe–2S] proteins is low; however, what homology is present is most evident in the loop which contains three of the four cysteinyl ligands for the prosthetic group (Pochapsky & Ye, 1991). It is not unreasonable, therefore, to use known [2Fe–2S] cluster geometries and ligation patterns observed in structures of other [2Fe–2S] proteins as models for preliminary structural calculations. These calculations are in progress, and as further constraints become available from stereospecific assignments and heteronuclear NMR studies, they will be incorporated in the constraint sets used for distance geometry/molecular dynamics analysis of the solution structure of Pdx (T. Branham and T. Pochapsky, unpublished results).

ACKNOWLEDGMENTS

We thank A. Redfield and his group for access to their spectrometer and assistance in its use. The LDB-500 is operated with funding from the NIH (GM-20168). Computational facilities were provided in part by a grant from the NIH (1-S10-RR0-4671-01). We thank S. Sligar (University of Illinois, Urbana) for stimulating discussion.

Registry No. Trp, 73-22-3.

REFERENCES

Bax, A., & Davis, D. G. (1985) *J. Magn. Reson. 65*, 355–360.

Bhasker, C. R., Okamura, T., Simpson, E. R., & Waterman, M. R. (1987) *Eur. J. Biochem. 164*, 21-26.
Billeter, M., Braun, W., & Wüthrich, K. (1982) *J. Mol. Biol. 155*, 321-346.
Cushman, D. W., Tsai, R. L., & Gunsalus, I. C. (1967) *Biochem. Biophys. Res. Commun. 26*, 577.
Davies, M. D., Qin, L., Beck, J. L., Suslick, K. S., Koga, H., Horiuchi, T., & Sligar, S. G. (1990) *J. Am. Chem. Soc. 112*, 7396-7398.
Gerber, N. C., Horiuchi, T., Koga, H. & Sligar, S. G., (1990) *Biochem. Biophys. Res. Commun. 169*, 1016.
Geren, L., Tuls, J., O'Brien, P., Millett, F., & Peterson, J. A. (1986) *J. Biol. Chem. 261*, 15491-15495.
Gunsalus, I. C., & Wagner, G. C. (1978) *Methods Enzymol. 52*, 166-188.
Koga, H., Yamaguchi, E., Matsunaga, K., Aramaki, H., & Horiuchi, T. (1989) *J. Biochem. (Tokyo) 106*, 831-836.
Kumar, A., Ernst, R. R., & Wüthrich, K. (1980) *Biochem. Biophys. Res. Commun. 95*, 1-6.
Lipscomb, J. D., Namtvedt, M. J., & Gunsalus, I. C. (1972) *Fed. Proc. 31*, 448.
Lipscomb, J. D., Sligar, S. G., Namtvedt, M. J., & Gunsalus, I. C. (1976) *J. Biol. Chem. 251*, 1116-1124.
Mathews, F. S., Argos, P., & Levine, M. (1971) *Cold Spring Harbor Symp. Quant. Biol. 36*, 387-395.
Oh, B.-H., & Markley, J. L. (1990) *Biochemistry 29*, 3993-4004.
Otting, G., & Wüthrich, K. (1986) *J. Magn. Reson. 66*, 359-363.
Otting, G., Widmer, H., Wagner, G., & Wüthrich, K. (1986) *J. Magn. Reson. 66*, 187-193.
Plateau, P., & Gueron, M. (1982) *J. Am. Chem. Soc. 104*, 7310-7311.
Pochapsky, T. C., & Ye, X. M. (1991) *Biochemistry 30*, 3850-3856.
Poulos, T. L., Finzel, B. C., Gunsalus, I. C., Wagner, G. C., & Kraut, J. (1985) *J. Biol. Chem. 260*, 16122.
Poulos, T. L., Finzel, B. C., & Howard, A. J. (1986) *Biochemistry 25*, 5314-5322.
Poulos, T. L., Finzel, B. C., & Howard, A. J. (1987) *J. Mol. Biol. 195*, 687-700.
Rance, M., Sorensen, O. W., Bodenhausen, G., Wagner, G., Ernst, R. R., & Wüthrich, K. (1983) *Biochem. Biophys. Res. Commun. 117*, 458-479.
Saudek, V., Wormald, M. R., Williams, R. J. P., Boyd, J., Stefani, M., & Ramponi, G. (1989) *J. Mol. Biol. 207*, 405-415.
Shiro, Y., Iizuka, T., Makino, R., Ishimura, Y., & Morishima, I. (1989) *J. Am. Chem. Soc. 111*, 7707-7711.
Sligar, S. G. (1976) *Biochemistry 15*, 5399.
Sligar, S. G., DeBrunner, P. G., Lipscomb, J. D., Namtvedt, M. J., & Gunsalus, I. C. (1974) *Proc. Natl. Acad. Sci. U.S.A. 71*, 3906-3910.
States, D. J., Haberkorn, R. A., & Ruben, D. J. (1982) *J. Magn. Reson. 48*, 741-751.
Stayton, P. S., & Sligar, S. G. (1990) *Biochemistry 29*, 7381-7386.
Stayton, P. S., Poulos, T. L., & Sligar, S. G. (1989) *Biochemistry 28*, 8201-8205.
Tyson, C. A., Tsai, R. L., & Gunsalus, I. C. (1972) *J. Biol. Chem. 247*, 5777.
Wüthrich, K. (1986) *NMR of Proteins and Nucleic Acids*, John Wiley and Sons, New York.

Inhibition of Phosphate Transport across the Human Erythrocyte Membrane by Chemical Modification of Sulfhydryl Groups

Takeo Yamaguchi* and Eiji Kimoto

Department of Chemistry, Faculty of Science, Fukuoka University, Jonan-ku, Fukuoka, Fukuoka 814-01, Japan

Received June 11, 1991; Revised Manuscript Received November 18, 1991

ABSTRACT: Effects of sulfhydryl-reactive reagents on phosphate transport across human erythrocyte membranes were examined using ^{31}P NMR. Phosphate transport was significantly inhibited in erythrocytes treated with sulfhydryl modifiers such as *N*-ethylmaleimide, diamide, and Cu^{2+}/*o*-phenanthroline. Quantitation of sulfhydryl groups in band 3 showed that the inhibition is closely associated with the decrease of sulfhydryl groups. Data from erythrocytes treated with diamide or Cu^{2+}/*o*-phenanthroline demonstrated that intermolecular cross-linking of band 3 by oxidation of a sulfhydryl group, perhaps Cys-201 or Cys-317, decreases the phosphate influx by about 10%. The inhibition was reversed by reduction using dithiothreitol. These results suggest that sulfhydryl groups in the cytoplasmic domain of band 3 may play an important role in the regulation of anion exchange across the membrane.

Human band 3 (M_r 101 791), composed of 911 amino acids (Lux et al., 1989), is the major intrinsic membrane protein of the erythrocyte which catalyzes a one-to-one exchange of anions across the plasma membrane (Passow, 1986). This glycoprotein is composed of two functionally distinct domains (Steck et al., 1976, 1978): a 43-kDa cytoplasmic domain which binds ankyrin (Hargreaves et al., 1980; Bennett & Stenbuck, 1980; Thevenin et al., 1989) and other cytoskeletal (Korsgren & Cohen, 1986) and cytosolic proteins (Strapazon & Steck, 1976), and the C-terminal transmembrane domain which spans the bilayer multiple times (Tanner et al., 1988; Lux et al., 1989).

Amino acids essential for anion transport activity in erythrocyte membranes have been examined using a variety

* To whom correspondence should be addressed.

0006-2960/92/0431-1968$03.00/0